CrossMark

ORIGINAL ARTICLE

Thermal distribution analysis of three-dimensional tumor-embedded breast models with different breast density compositions

Asnida Abd Wahab[1] · Maheza Irna Mohamad Salim[1] ·
Mohamad Asmidzam Ahamat[2] · Noraida Abd Manaf[1] · Jasmy Yunus[1] · Khin Wee Lai[3]

Abstract Breast cancer is the most common cancer among women globally, and the number of young women diagnosed with this disease is gradually increasing over the years. Mammography is the current gold-standard technique although it is known to be less sensitive in detecting tumors in woman with dense breast tissue. Detecting an early-stage tumor in young women is very crucial for better survival chance and treatment. The thermography technique has the capability to provide an additional functional information on physiological changes to mammography by describing thermal and vascular properties of the tissues. Studies on breast thermography have been carried out to improve the accuracy level of the thermography technique in various perspectives. However, the limitation of gathering women affected by cancer in different age groups had necessitated this comprehensive study which is aimed to investigate the effect of different density levels on the surface temperature distribution profile of the breast models. These models, namely extremely dense (ED), heterogeneously dense (HD), scattered fibroglandular (SF), and predominantly fatty (PF), with embedded tumors were developed using the finite element method. A conventional Pennes' bioheat model was used to perform the numerical simulation on different case studies, and the results obtained were then compared using a hypothesis statistical analysis method to the reference breast model developed previously. The results obtained show that ED, SF, and PF breast models had significant mean differences in surface temperature profile with a p value <0.025, while HD breast model data pair agreed with the null hypothesis formulated due to the comparable tissue composition percentage to the reference model. The findings suggested that various breast density levels should be considered as a contributing factor to the surface thermal distribution profile alteration in both breast cancer detection and analysis when using the thermography technique.

Keywords Breast cancer simulation · Surface temperature profile · Thermography · Breast density

✉ Maheza Irna Mohamad Salim
maheza@biomedical.utm.my

Asnida Abd Wahab
asnida.abd.wahab@gmail.com

[1] Faculty of Biosciences and Medical Engineering, University of Technology Malaysia, 81310 Johor Bahru, Malaysia

[2] Thermal Fluid Unit, HVACR Section, Malaysia France Institute, University of Kuala Lumpur, 43650 Selangor, Malaysia

[3] Department of Biomedical Engineering, Faculty of Engineering, University of Malaya, 51310 Kuala Lumpur, Malaysia

1 Introduction

The number of breast cancer incidences has risen at a very significant scale, and it has appeared to be the second leading cause of death in women [2]. Current research also show that the number of young women diagnosed with breast cancer has increased concurrently [10, 11, 37]. On the other hand, studies also show that early detection and treatment of cancer can lead to higher survival chance compared to late detection [12, 16].

These important findings indicate that detecting breast cancer at its earliest stages is very crucial to saving lives. To date, mammography has still remains as the gold-standard technique for breast cancer imaging worldwide. However, routine mammography is only recommended for women of 40 years old and above since the effectiveness of

mammography decreases for higher density level of breast tissue in young women [20, 50, 52, 57]. This is because X-rays permeate through different types of breast tissues differently. It has been discovered that high-density breast tissues attenuate the X-ray radiation to a greater extent compared to fatty tissue and appear as a relatively lighter area, thus causing reduction in both sensitivity and specificity of the mammography [13].

Breasts are made from the combination of ducts, lobules or glandular, fatty, and fibrous connective tissues. The breasts of women are considered dense if they have a higher composition of fibrous and connective tissues with low fatty tissue content, while the breasts are considered less dense when the fatty tissue composition is high. Generally, the density level of the breasts decreases with age, and based on the Breast Imaging Reporting and Data System (BI-RADS) developed by American Cancer Research, breast density can be divided into four main categories: extremely dense (ED), heterogeneously dense (HD), scattered fatty (SF), and predominantly fatty (PF) [13, 45]. Younger women tend to have denser breasts, and previous studies have shown that women with dense breasts have a four-to-sixfold increased risk of developing breast cancer [10, 13, 28]. Hence, the breast density factor should be considered when evaluating the potential benefits of extended imaging from breast cancer screening [14, 28]. These studies concluded that a reliable technique for early detection of cancer in young women with high breast density is indeed very crucial for a better survival rate.

Multiple adjunctive screening tools such as elastography, electrical impedance tomography (EIT), and diffuse optical imaging (DOI) techniques have been developed to be used alongside mammography techniques in detecting early stages of tumor in young women [27, 32, 38, 39, 51, 53, 59]. Thermography imaging technique has shown to be a potential screening tool with a higher level of sensitivity in complementing the current gold-standard technique [35]. It is a non-invasive and harmless imaging technique, which requires no breast compression and is cost-effective and free from any radiation [5, 23, 29]. A comparative study between thermography and other imaging modalities, specifically for breast cancer imaging, has proven that thermography provides additional functional and physiological information on thermal and vascular properties of the tissues [32]. On the other hand, Gautherie and Gros, in their twelve years of cancer thermographic study on breast cancer patients, showed that thermography is useful as a risk factor predictor and also to assess rapidly growing neoplasm [24]. Hence, many studies have been carried out to improve the accuracy of thermography as an adjunctive tool in early detection of breast cancer [22, 25, 38, 40, 44, 48, 56, 58, 61].

Different tissues have different thermal conductivity values, which elevate the core body temperature at various rates [62]. Both cancerous and pre-cancerous tissues have high metabolic rates due to their rapid multiplication, which demand more blood vessels in order to supply sufficient nutrients to these fast growing cells [5, 23, 26]. This process is called angiogenesis, which will consequently elevate the temperature of the surrounding tissues, causing skin surface temperature alteration via heat conduction and convection processes occurring within the tissues and blood vessels, respectively. Hence, thermography uses this heat information, which is radiated from the skin surface in infrared thermal radiation form to be converted into an energy signal and calculated using different parameters to map the actual surface temperature of an object in a simplified visual format also known as a thermogram.

Current studies on breast thermography have also shown that thermography is not yet fully accepted for an adoption into a clinical practice due to lack of screening data on asymptomatic population as well as having a limitation in obtaining breast cancer patients from different age groups, especially in young women [6, 59]. Bezerra and others, in their clinical studies, have revealed that the estimated values of parameters from their simplified physical model was worse compared to those results obtained from two actual patients, a young woman and an old woman, respectively. They concluded that this was probably due to the age of the patients who had different physical breast properties and density levels compared to their homogeneous model [8]. Furthermore, several breast models developed previously for numerical simulation and analysis purposes have either used single-layer tissue breast models (two- and three-dimensional), homogeneous phantoms, or a single composition multi-layer breast model [1, 3, 17, 18, 36, 58]. Besides, the complexity of human breast tissue composition has resulted in minimal progressive in the investigation of breast density level as a contributing factor in thermal profile alteration.

Meanwhile, in a series of studies conducted by Ng and Sudarshan, a single flexible multi-layer four-quadrant breast model has been developed to analyze the effects of blood flow and tumor existence on female breasts using finite element method (FEM) simulation. This model allowed the authors to mold the model based on the required pattern with proper choice of tissue properties values. They concluded that metabolic heat generation and blood perfusion properties are the key parameters that affected the skin surface temperature, whereas lowering these factors at the minimal levels maximized the effective heat transfer process [40–42]. They also highlighted that the large variability in breast diameter and tissue volume would affect the magnitude of temperature profile, but no further analysis was carried out

Table 1 Tissue composition percentage and thermo-physical parameters for all breast models

Tissue composition (%)	Muscle (D_1)	Gland (D_2)	Fat (D_3)	Tumor (T_1)
Extremely dense (ED)	20	70	10	–
Heterogeneously dense (HD)	20	60	20	–
Scattered fibroglandular (SF)	20	40	40	–
Predominantly fatty (PF)	10	20	70	–
Ng and Sudharsan	26.5	54.1	19.4	–
Thermophysical parameters	Muscle (D_1)	Gland (D_2)	Fat (D_3)	Tumor (T_1)
Thermal conductivity (W/m °C)	0.48	0.48	0.21	0.48
Metabolic heat generation (W/m^3)	700	700	400	8720
Blood perfusion (1/s)	0.8e−3	0.5e−3	0.2e−3	0.1e−1
Specific heat blood (J/kg °C)	4200	4200	4200	4200
Blood density (kg/m^3)	1060	1060	1060	1060

to specifically address this issue [54]. On the other hand, Li and others have developed a three-dimensional FEM breast model associated with both thermal and elastic properties of the breast. The effects of both properties to the surface temperature distribution were quantitatively investigated, and this fused model was found to be very useful in enhancing the clinical application foundations of breast thermography [30, 31]. In addition, Das and Mishra, in their recent studies, have developed a simplified homogeneous two-dimensional breast model in estimating the size and the location of tumor. Nonetheless, they did not consider certain factors, such as multi-layers tissue or breast density, since the analysis of these parameters estimation would increase computational time [18, 19]. Next, Mital and Pidarpati have adopted the multi-layer breast model from Ng and Sudarshan and investigated tumor parameters using an evolutionary algorithm. They suggested that a non-uniform 3D breast geometry should be considered in future investigation to be used in a clinical scenario although its complexity and computational time may increase [36]. Hence, it can be seen that due to the complexity of modeling realistic breast model with different breast density levels, many previous studies have excluded this factor as part of their aim and methodology.

Therefore, the objective of this particular study was to develop breast models with different breast density levels and to investigate the effects of changes in varying breast density compositions to the surface temperature distribution profile of the breast. Four different breast models that were comprised of different breast density levels with embedded tumors were developed, and a statistical analysis of four different case studies was conducted to observe the mean difference in comparison with the existing model developed by Ng and Sudarshan [34, 40, 41].

2 Methods

2.1 Breast modeling

Four different three-dimensional breast models, namely extremely dense (ED), heterogeneously dense (HD), scattered fatty (SF), and predominantly fatty (PF), with different breast density compositions (Table 1) were developed based on the multi-layer configuration breast model presented by Ng and Sudharsan [41]. The tissue compositions ratio was adopted according to the Breast Imaging Reporting and Data System (BI-RADS) developed by America Cancer Research [7]. In addition, inverse calculation was performed by converting the dimension values given in the reference model into the percentage of tissue compositions for each layer as tabulated in Table 1.

Figure 1 shows the cross-sectional view of the developed breast models which are comprised of muscle layer (DI), glandular layer (D2), and subcutaneous fat layer (D3). Anatomically, glandular layer consist of lobules, lactiferous ducts, and fibrous tissue. The tumor is shown as T_1 which was embedded in the centerline of the breast model to minimize the effect of the asymmetrical tissue thickness due to the curvature nature of the breast. In addition, the breast model properties were constructed to be as close as possible to the actual breast anatomy in order to perform a good and smooth numerical simulation to mimic human physiological changes [42, 56]. A homogeneous spatial distribution of blood vessels is assumed in all tissue components, in order to minimize the heterogeneity effects on the overall surface temperature profile.

A hemispherical shape with a diameter $L = 14.4$ cm was used to represent the average female breast geometry [41, 47, 48]. Meanwhile, the glandular layer was developed by using another hemispherical shape with a smaller
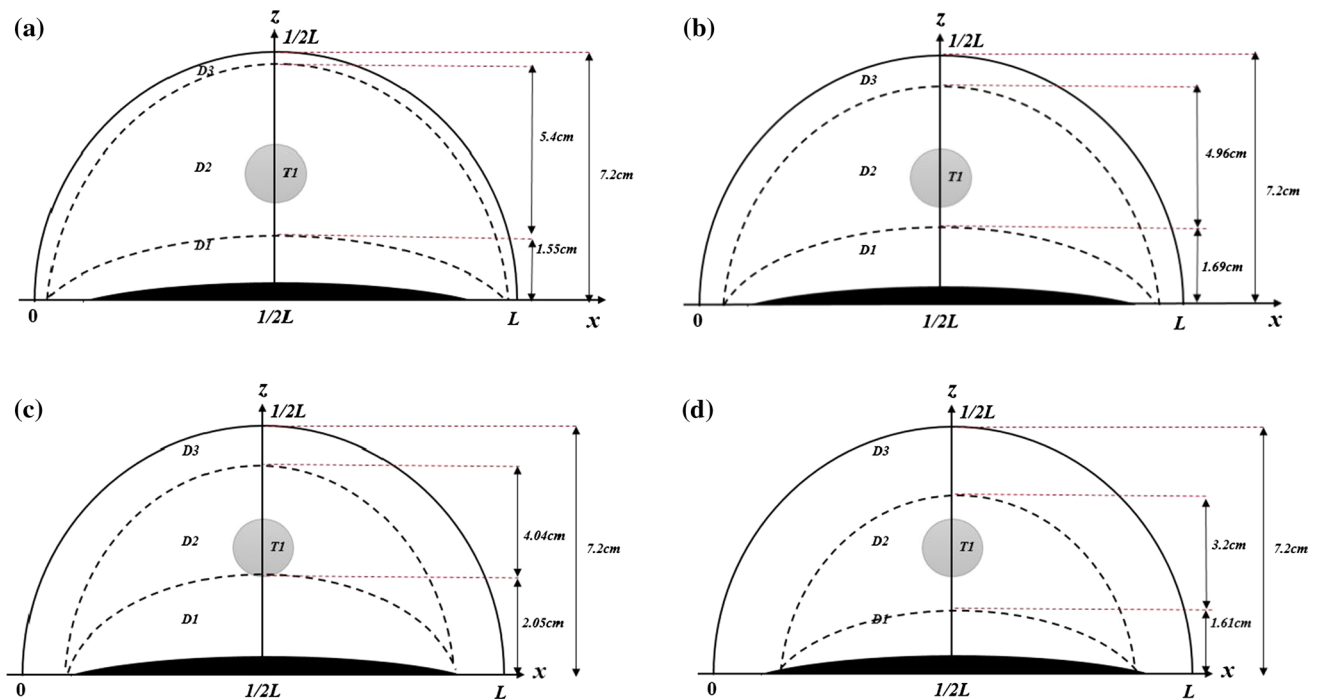
Fig. 1 Cross-sectional view of breast models with different breast compositions, **a** ED, **b** HD, **c** SF and **d** PF

radius and a semi-ellipsoidal shape with specified radius and height to mimic the muscle layer. The dimension of the thoracic wall underneath the muscle layer was consistently maintained to ensure that the breast model had a constant volume throughout the study. A perfect spherical shape with size range of 1.0–3.0 cm was embedded in the breast model to mimic the in situ tumor with a constant diameter to represent the small non-palpable tumor, which was classified clinically as T_1 and T_2 at the international level to denote the early stages (Stage 0 and Stage I) of tumor characteristics [41].

2.2 Bioheat transfer mechanism

Heat transfer in living tissue is a complicated and complex biological process involving multiple mechanisms, such as heat conduction, heat convection by blood perfusion, and metabolism. One of the functions of blood flow in the biological system is to provide thermal stability to the tissue, depending on the relative local tissue temperature. Moreover, in a biomedical environment, any abnormality and sudden change in temperature distribution can be intrinsically connected to both biological and physiological processes, and they are normally the first signs of a disease [19]. This behavior is closely related to the cancerous tissue. This is because the rapid growth of cancer cells would require sufficient nutrient supply that would be transported through blood vessels. The newly formed

blood vessel known as angiogenesis would subsequently increase the metabolic rate of the surrounding tissues, and these changes would eventually induce temperature alteration on the skin surface via heat conduction and convection processes occurring within the tissues and blood vessels, respectively [4, 5, 33].

2.3 Thermophysical properties and numerical simulation

The numerical simulation of these breast models was performed via the finite element method (FEM) available in COMSOL Multiphysics computational package. A set of thermophysical parameters was used in the simulation for different types of tissue layers as shown in Table 1 [24, 60]. Next, each breast model was meshed into a predefined number of finite elements as the first step of FEM for spatial discretization. The tetrahedral meshing was selected. Test on normal and fine element size meshing settings showed that the difference in surface temperature was insignificant. Therefore, in order to reduce the computational time, a normal element size meshing has been adopted to all domains for simulation.

According to Gautherie in his extensive study, the tumor doubling time and the metabolic rate can be related by a hyperbolic function, as shown in Eq. (1), while the tumor diameter related to the doubling time can be expressed as Eq. (2) [24].
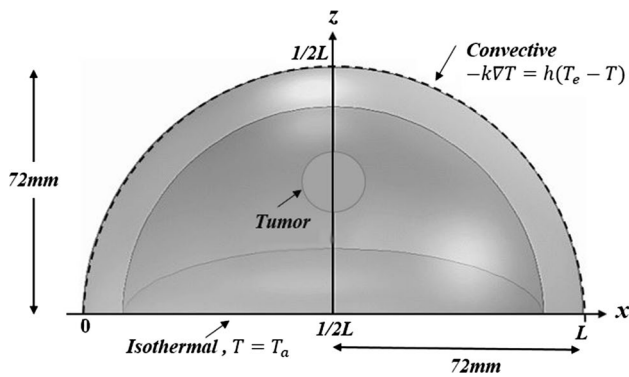
Fig. 2 Boundary condition adopted for the breast model

$$q_{\mathrm{m}}\tau = C\left(\mathrm{W\ day/m}^3\right) \tag{1}$$

$$D = \mathrm{e}^{(0.002134 \times (\tau - 50))} \times 10^{-2}\ \mathrm{m} \tag{2}$$

where $C = 3.27 \times 10^6$ W day/m^3 and τ is the volume doubling time of the tumor. Hence, based on both equations above, it was possible to calculate the respective metabolic heat value for different tumor sizes. Therefore, metabolic heat generation, q_{m} for tumor size of 1.0, 2.0, and 3.0 was $65.4 \times 10^3, 8.72 \times 10^3$ and 5.79×10^3 W/m^3, while the calculated doubling days were approximately 50, 375, and 564 days, respectively.

In this study, Pennes' bioheat equation (PBHE) was adopted to model the heat transfer mechanism in the blood-perfused tissues and to quantitatively describe the thermal interaction in the breast on a continuum basis [49]. Equation 3 describes the steady state of heat transfer via conduction through the tissue, as the volumetric metabolic heat generation of the tissue was considered to be directly proportional to the product of the volumetric perfusion rate, as well as the temperature difference between the arterial blood and the local tissue.

$$\nabla \cdot (-k\nabla T) = \rho_{\mathrm{b}}\omega_{\mathrm{b}}c_{\mathrm{b}}(T_{\mathrm{a}} - T) + q_{\mathrm{m}} \tag{3}$$

where ω_{b}, ρ_{b}, and c_{b} are the perfusion rate, the density, and the specific heat capacity of the blood. T is the local tissue temperature, T_{a} is the arterial blood temperature, and q_{m} represents the metabolic heat generation rate.

Additionally, Fig. 2 shows the boundary conditions adopted to all breast models are specified at the breast skin surface as shown in Eq. 4:

$$-k\nabla T = h(T_{\mathrm{e}} - T) \tag{4}$$

where T_{e} is the surrounding temperature and h represents the combined effective heat transfer coefficient due to convection, radiation, and evaporation of 13.5 W/m^2 K [47, 48, 55]. The inner boundary condition at the core area of the

thoracic wall was considered to be adiabatic and isothermal with a fixed temperature of 37 °C. Four case studies were carried out on each of the breast model with a total of 85 separate cases of simulation performed. Case study (i) was designed to observe the baseline surface temperature of healthy breast in all models without any presence of tumor. Case study (ii) was designed to monitor the effect of different tumor locations on surface temperature profiles by embedding a fixed tumor size of 2 cm throughout the simulation. In case study (iii) and (iv), two locations specifically 5.5 and 4.5 cm from body core were selected, respectively, to observe the effect of various tumor sizes on surface temperature profile.

Finally, a statistical analysis of the surface temperature mean difference for all breast models based on case study (ii) and (iii) was performed to quantify whether various breast densities have a significant influence to the overall surface mean temperature difference when compared to the reference model. The null hypothesis, H_0, was formulated where the mean temperature of the reference breast model had insignificant difference compared to other breast models developed, i.e., $H_{0:}$ $\mu_{\mathrm{ref}} = \mu_x$, where x represents ED, HD, SF, and PF breast models individually. Since both groups involved were independent of each other, an unpaired two-tailed t test analysis with 95 % confidence interval (CI) was employed in this study to calculate the probability of the observing data obtained, as well as to determine whether they agreed with the null hypothesis statement. The test was carried out on all case studies, and the probability of the data pair was observed.

3 Results

3.1 Surface temperature profile analysis

Figure 3 shows the result of the surface temperature profile for a normal breast model. It was observed that for normal breast model simulation, the maximum surface temperature for the ED breast model was the highest among all, followed by Ng and Sudharsan's breast model, the HD breast model, SF breast model, and PF breast model, respectively. As depicted in Table 1, tissue composition percentage of the reference and the HD models was almost similar, and hence, their surface temperature distribution shifted only by approximately 1.1 °C compared to other models.

On the other hand, Fig. 4 shows the maximum surface temperature profile of a tumor with a diameter of 2.0 cm embedded in 6 different locations which represents case study (ii). Generally, each model displayed a Gaussian distribution profile since all models were developed using a symmetrical geometry measurement. As the tumor moves closer to the surface, the increase in the maximum surface

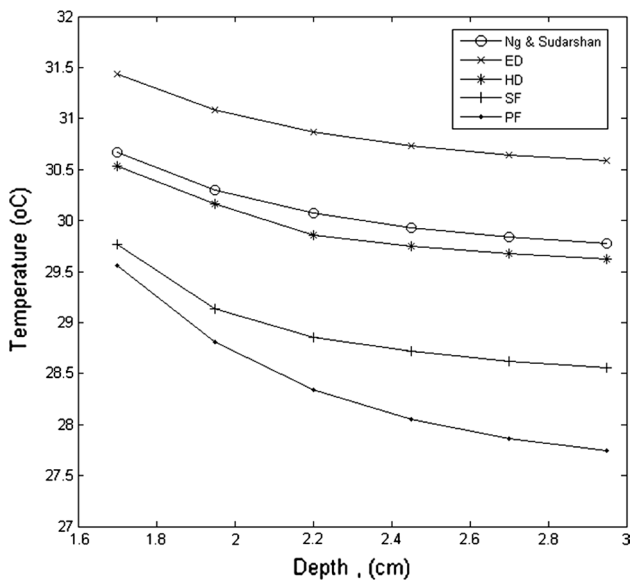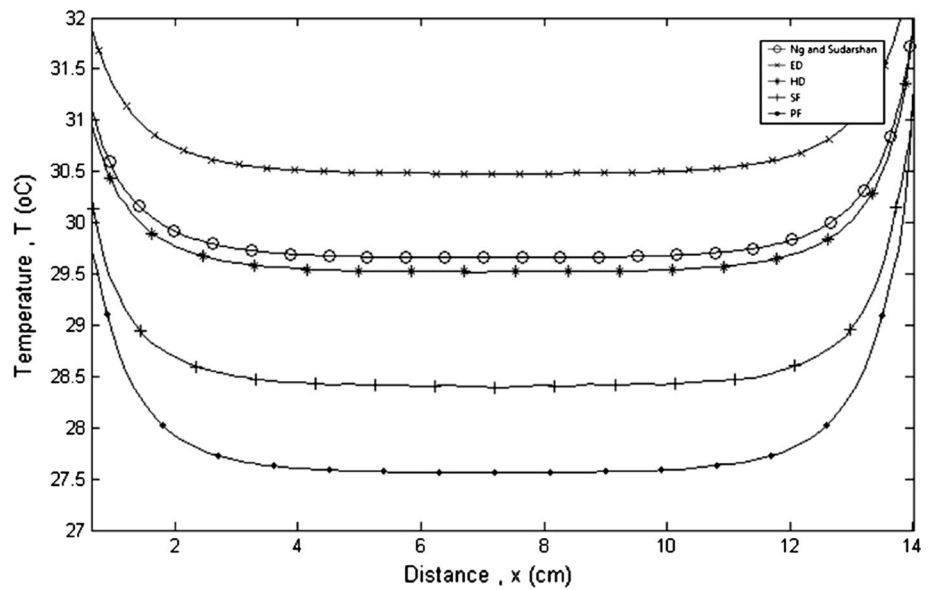Fig. 3 Surface temperature profile for healthy breast models

Fig. 4 Maximum surface temperature for tumor size of 2.0 cm at various depth locations
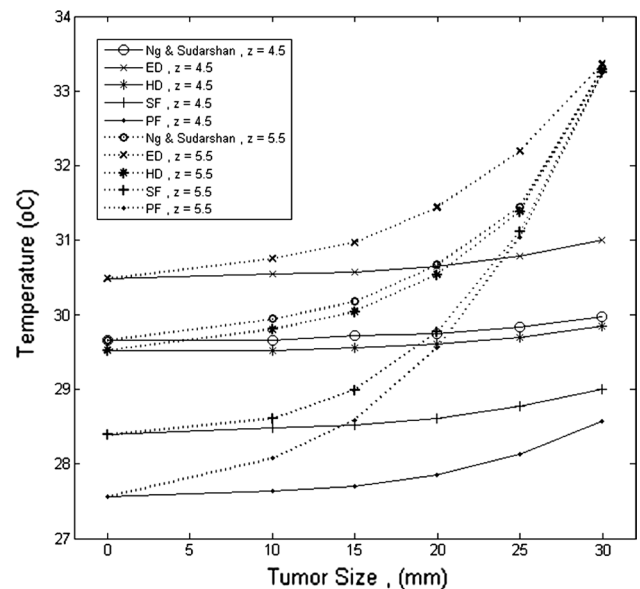

Fig. 5 Maximum surface temperature of various tumor sizes at two locations (i) 4.5 cm and (ii) 5.5 cm from body core

temperature became more significant for both SF and PF breast models with 1.3 and 1.9 °C, respectively, compared to the case where the tumor was located far from the breast surface. At $z = 5.5$ cm (1.7 cm from surface), both maximum surface temperatures for SF and PF breast models had a slight difference of 0.2 °C compared to the earlier case where the tumor was positioned at $z = 4.5$ cm (2.7 cm from surface) and its maximum temperature difference was 0.7 °C. However, as for ED and HD breast models, their temperature increment patterns were comparable as they portrayed approximately 1 °C difference from their normal breast models. Hence, this showed that for a tumor located

closer to the breast surface, all models experienced a significant temperature increase from their normal and healthy breast models, but when the tumor location was farther from the breast surface, their surface temperature increase was quite a challenge to be detected, especially in SF and PF, due to their overall low surface temperature. This could eventually result in a misinterpretation of the thermogram.

From case study (ii), 2 locations have been chosen to represent both superficial and deeper locations which were then adopted in case study (iii) and case study (iv), respectively. Figure 5 shows the simulation results of all models with various tumor sizes located at $z = 5.5$ cm and

Table 2 Results of t test analysis for all models developed against the reference model for case study (ii)

Tumor location (cm)	t test	ED	HD	SF	PF
5.50	p value	0.0001	0.1919	0.0001	0.0001
	t value	6.1146	1.3069	9.0924	13.9724
	Df	588	474	442	442
5.25	p value	0.0001	0.2304	0.0001	0.0001
	t value	6.0318	1.2008	9.3652	13.8655
	Df	588	458	442	426
5.00	p value	0.0001	0.2292	0.0001	0.0001
	t value	21.7117	1.2039	8.9242	14.1737
	Df	482	458	426	426
4.75	p value	0.0001	0.2333	0.0001	0.0001
	t value	5.8982	1.1935	8.6978	14.1395
	Df	588	458	426	426
4.50	p value	0.0001	0.2333	0.0001	0.0001
	t value	5.8578	1.1935	8.6733	14.1608
	Df	588	458	426	426

Table 3 Results of t test analysis for all models developed against the reference model for case study (iii)

Tumor size (cm)	t test	E	HD	SF	PF
1.0	p value	0.0001	0.2109	0.0001	0.0001
	t value	5.8193	1.2527	8.8604	14.8579
	df	588	458	426	442
1.5	p value	0.0001	0.2122	0.0001	0.0001
	t value	5.945	1.2493	9.2954	14.5347
	df	588	458	442	442
2.0	p value	0.0001	0.1919	0.0001	0.0001
	t value	6.1146	1.3069	9.0924	13.9724
	df	588	474	442	442
2.5	p value	0.0001	0.1177	0.0001	0.0001
	t value	6.0158	1.5672	8.9367	13.5774
	df	630	532	484	484

$z = 4.5$ cm from body core. These case studies were carried out to observe the changes in surface temperature profile in the breast models as the tumor's size changes or grows. It was observed that as the tumor size increased from 1.0 to 3.0 cm, the maximum surface temperature of all models in both locations increased accordingly. However, for a tumor located at $z = 5.5$ cm, it can be seen that as the tumor grew to the maximum size and approaching the surface, all models have shown to have significant maximum temperature increase and had an approximately similar temperature value. While for a tumor size of 3.0 cm located at $z = 4.5$ cm, the maximum temperature differences between each models can be clearly distinguished with minimal temperature distribution alteration where the ED model

showed a higher maximum temperature from the reference model, HD breast model had the closest increase pattern with 0.1 °C difference from reference model while both SF and PF models had lower maximum surface temperature compared to the reference model by 0.98 and 1.41 °C, respectively. Finally, it can also be seen that the surface temperature profile for breast models with tumor size of 1.0 cm located at $z = 4.5$ cm had shown to be qualitatively similar from their initial normal healthy condition. However, by quantitative measurement, their temperature values have shown to increase at a minimal range compared to a larger tumor located as the same location.

3.2 Statistical analysis for temperature mean difference

Tables 2 and 3 show the results from case studies (ii) and (iii), respectively. The results obtained from two-tailed t test analysis are usually expressed as $t(df) = t$ value, p value <0.025 where t value indicates the t statistic, p value indicates the probability of obtaining the given t value by chance alone, and df is the degree of freedom. It can be clearly observed from Table 2 that ED, SF, and PF breast models had p values <0.05 for all tumor locations and sizes. Thus, ED, SF, and PF breast models had shown to be statistically significant toward the reference model due to the difference breast compositions percentage, which provided strong evidence against the null hypothesis developed in this study. On the other hand, the result for the surface temperature mean difference between HD and reference breast models showed that the two-tailed p value was statistically insignificant in both case studies. This is because, the ratio of tissue composition in HD model developed had the closest percentage value compared to the reference model as shown in Table 1.

4 Discussion

The overall finding was supported by Chen and Holmes, who in their studies stated that besides perfusion heating, thermal conductivity is another factor that contributes to the heat transfer process in the tissue [15]. Since the metabolic heat generation and thermal conductivity values of the gland are higher compared to the fatty tissue, the biological heat conductivity process in the dense breast tissue is more effective than the less dense breast which results in higher overall temperature alteration on the skin surface. Thus, the breast density factor shows to be crucial when estimating tumor parameters.

The maximum temperature distribution profile from case study (ii) revealed the effects of different tumor locations to average surface temperature profile. It can be seen that as the tumor moves closer to the skin surface, SF and

PF models were shown to have higher temperature differences compared to the other models. Although significant differences are normally translated as an increase in sensitivity, in reality additional surrounding convective heat transfer could reduce the physical breast surface temperature and make detecting deeper tumor in low-dense breast more challenging and less sensitive [46].

In addition, Fig. 5 has shown that for tumor size of 3.0 cm at $z = 5.5$ cm which was positioned underneath the skin surface, all breast models showed approximately similar maximum temperature points. This was due to the thin layer of fat tissue that separated the tumor in all models before it ulcerated or penetrated through the skin surface which can be easily detected and palpated via a clinical breast examination (CBE) procedure. Thus, at this location, the tumor possessed higher effects on the maximum surface temperature alteration in all models, while tissue density was proven to have less effect on the warmer area but only to the surrounding healthy tissue. However, the increase in the temperature values was based on the models developed, and they could possibly have a various increment patterns when the tissues are arranged differently, which is one of the challenges faced by researchers in modeling real breasts since every woman has varying physical breast properties [9, 41, 43, 54]. Nevertheless, the ED breast model shown higher maximum surface temperature than the other models when the size of the tumor was less than 2.0 cm. Thus, it is equally important to compare the surface temperature value for both breasts in order to obtain their surface temperature profile, especially in detecting smaller or farther underlying tumors that cannot be palpated via a CBE procedure or via mammography.

Although changes in tumor sizes and locations altered the surface temperature profile, case studies (ii), (iii), and (iv) have shown that tumor location from the skin surface had a higher effect on the surface temperature profile alteration compared to its size, even though smaller tumor tended to have a higher metabolic rate. In fact, a similar observation was made by Das and others in their previous study [17]. Hence, the overall observation indicates that if the tumor parameter estimation is calculated without considering the breast density level factor and other tissue properties [48, 54], one might over estimate the size or the actual location of the tumor from the thermogram obtained.

Finally, based on the statistical analysis conducted, it was proven that with the presence of tumor, different breast density models showed significant alterations in surface temperature profile in addition to other parameters, such as blood perfusion and metabolic heat generation [21, 40]. The breast density level factor, which can be directly related to age, depicted that a single-layer or a single breast composition model is insufficient to represent a model for women's breasts in general [14]. However, by considering multiple breast density models, researchers could estimate tumor size, locations, and other thermophysical properties with a better accuracy since there is no specific breast model that can fit all breast types.

5 Conclusion

The simulation results obtained showed that different breast densities produced varying surface temperature distribution profiles with the presence of tumor. Quantitatively, statistical analysis revealed that ED, SF, and PF breast models had significant surface temperature mean differences from the reference model with p value >0.025 in all simulation results, while HD breast model contrarily showed insignificant surface temperature mean difference from the reference model. This statistical analysis is very important to provide evidence that breast density level is indeed a factor that contributes to the significant alteration of the surface temperature profile for cancerous breasts.

Furthermore, it was also observed that as the tumor moved toward the skin surface, all models had approximately similar maximum surface temperatures. At this point, breast density levels failed in providing a distinguishable maximum temperature for all models, but required a comparison of both breasts to obtain the maximum temperature difference with their normal healthy breast. However, as the tumor becomes superficial, it can normally be easily detected via a CBE procedure, and thus, thermography screening may not be necessary. Hence, this study suggested that the breast density factor should be considered for smaller and deeper tumor cases among young women with dense breasts. For future study, dynamic thermal changes should be observed and tumor locations should be varied on all axes in order to observe the asymmetrical surface temperature profile for all breast models with varying tissue arrangements. As for this study, the heat convection was maintained at the same value, but one should consider the effect of overall heat boundary condition, especially in clinical practice, since it will cause further temperature degradation and different thermal alteration profiles on the skin surface.

In addition, although a large-scale data are still required to obtain a better standard for different breast density levels, this particular study hoped to facilitate the understanding of the complex mechanism underlying the observed surface temperature profile, as well as to improve the current early tumor detection and analysis for the thermography technique.

of Breast Cancer" and also to the Malaysian Ministry of Higher Education (MOHE) for providing the MyBrain scholarship.

References

1. Agnelli JP, Barrea AA, Turner CV (2011) Tumor location and parameter estimation by thermography. Math Comput Model 53:1527–1534

2. American Cancer Society (2013) Cancer facts and figures. American Cancer Society, New York

3. Amri A, Saidane A, Pulko S (2011) Thermal analysis of a three-dimensional breast model with embedded tumour using the transmission line matrix (TLM) method. Comput Biol Med 41:76–86

4. Anbar M (1994) Hyperthermia of the cancerous breast: analysis of mechanism. Cancer Lett 84:23–29

5. Arena F, Barone C, DiCicco T (2003) Use of digital infrared imaging in enhanced breast cancer detection and monitoring of the clinical response to treatment. In: Proceedings of 25th Annual International Conference on IEEE Engineering in Medicine and Biology Socirty (IEEE Cat. No. 03CH37439) vol 2

6. Arora N, Martins D, Ruggerio D, Tousimis E et al (2008) Effectiveness of a noninvasive digital infrared thermal imaging system in the detection of breast cancer. Am J Surg 196:523–526

7. Balleyguier C, Bidault F, Mathieu MC, Ayadi S et al (2007) BIRADS™ mammography: exercises. Eur J Radiol 61:195–201

8. Bezerra LA, Oliveira MM, Rolim TL, Conci A et al (2013) Estimation of breast tumor thermal properties using infrared images. Signal Process 93:2851–2863

9. Borchartt TB, Conci A, Lima RCF, Resmini R, Sanchez A (2013) Breast thermography from an image processing viewpoint: a survey. Signal Process 93:2785–2803

10. Boyd NF, Byng JW, Jong RA, Fishell EK et al (1995) Quantitative classification of mammographic densities and breast cancer risk: results from the Canadian National Breast Screening Study. J Natl Cancer Inst 87:670–675

11. Boyd NF, Martin LJ, Sun L, Guo H et al (2006) Body size, mammographic density, and breast cancer risk. Cancer Epidemiol Biomarkers Prev 15:2086–2092

12. Boyd NF, Guo H, Martin LJ, Sun L et al (2007) Mammographic density and the risk and detection of breast cancer. N Engl J Med 356:227–236

13. Boyd NF, Martin LJ, Bronskill M, Yaffe MJ et al (2010) Breast tissue composition and susceptibility to breast cancer. J Natl Cancer Inst 102:1224–1237

14. Checka CM, Chun JE, Schnabel FR, Lee J, Toth H (2012) The relationship of mammographic density and age: implications for breast cancer screening. Am J Roentgenol 198:292–295

15. Chen MM, Holmes KR (1980) Microvascular contributions in tissue heat transfer. Ann NY Acad Sci 335:137–150

16. Coleman MP, Quaresma M, Berrino F, Lutz JM et al (2008) Cancer survival in five continents: a worldwide population-based study (CONCORD). Lancet Oncol 9:730–756

17. Das K, Mishra SC (2013) Estimation of tumor characteristics in a breast tissue with known skin surface temperature. J Therm Biol 38:311–317

18. Das K, Mishra SC (2014) Non-invasive estimation of size and location of a tumor in a human breast using a curve fitting technique. Int Commun Heat Mass Transf 56:63–70

19. Das K, Singh R, Mishra SC (2013) Numerical analysis for determination of the presence of a tumor and estimation of its size and location in a tissue. J Therm Biol 38:32–40

20. de González AB, Reeves G (2005) Mammographic screening before age 50 years in the UK: comparison of the radiation risks with the mortality benefits. Br J Cancer 93:590–596

21. Dos Santos I, Haemmerich D, Pinheiro CDS, da Rocha AF (2008) Effect of variable heat transfer coefficient on tissue temperature next to a large vessel during radiofrequency tumor ablation. Biomed Eng Online 7:21

22. EtehadTavakol M, Lucas C, Sadri S, Ng EYK (2010) Analysis of breast thermography using fractal dimension to establish possible difference between malignant and benign patterns. J Healthc Eng 1:27–44

23. Foster KR (1998) Thermographic detection of breast cancer. IEEE Eng Med Biol Mag 17(6):10–14

24. Gautherie M (1980) Thermopathology of breast cancer: measurement and analysis. Ann NY Acad Sci 335:383–415

25. González FJ (2011) Non-invasive estimation of the metabolic heat production of breast tumors using digital infrared imaging. Quant Infrared Thermogr J 8:139–148

26. Gros C, Gautherie M, Bourjat P (1975) Prognosis and post-therapeutic follow-up of breast cancers by thermography. Bibl Radiol 77–90

27. Guo Y, Sivaramakrishna R, Lu CC, Suri JS, Laxminarayan S (2006) Breast image registration techniques: a survey. Med Biol Eng Comput 44:15–26

28. Harvey JA, Bovbjerg VE (2004) Quantitative assessment of mammographic breast density: relationship with breast cancer risk. Radiology 230:29–41

29. Head JF, Wang F, Lipari CA, Elliott RL (2000) The important role of infrared imaging in breast cancer. IEEE Eng Med Biol Mag 19:52–57

30. Jiang L, Zhan W, Loew MH (2008) Lector Notes on Computer Science (including Subser. Lect. Notes Artif. Intell. Lect. Notes Bioinformatics), vol 5242 LNCS, pp 798–805

31. Jiang L, Zhan W, Loew MH (2011) Modeling static and dynamic thermography of the human breast under elastic deformation. Phys Med Biol 56:187–202

32. Kennedy DA, Lee T, Seely D (2009) A comparative review of thermography as a breast cancer screening technique. Integr Cancer Ther 8:9–16

33. Kontos M, Wilson R, Fentiman I (2011) Digital infrared thermal imaging (DITI) of breast lesions: sensitivity and specificity of detection of primary breast cancers. Clin Radiol 66:536–539

34. Kotsianos-Hermle D, Hiltawsky KM, Wirth S, Fischer T et al (2009) Analysis of 107 breast lesions with automated 3D ultrasound and comparison with mammography and manual ultrasound. Eur J Radiol 71:109–115

35. Lahiri BB, Bagavathiappan S, Jayakumar T, Philip J (2012) Medical applications of infrared thermography: a review. Infrared Phys Technol 55:221–235

36. Mital M, Pidaparti RM (2008) Breast tumor simulation and parameters estimation using evolutionary algorithms. Model Simul Eng 2008:1–6

37. Nagao Y, Kawaguchi Y, Sugiyama Y, Saji S, Kashiki Y (2003) Relationship between mammographic density and the risk of breast cancer in Japanese women: a case–control study. Breast Cancer 10:228–233

38. Ng EYK, Kee EC (2008) Advanced integrated technique in breast cancer thermography. J Med Eng Technol 32:103–114

39. Ng EYK, Ng WK (2006) Parametric study of the biopotential equation for breast tumour identification using ANOVA and Taguchi method. Med Biol Eng Comput 44:131–139

40. Ng EYK, Sudharsan NM (2001) Effect of blood flow, tumour and cold stress in a female breast: a novel time-accurate computer simulation. Proc Inst Mech Eng Part H J Eng Med 215:393–404

41. Ng EYK, Sudharsan NM (2001) An improved three-dimensional direct numerical modelling and thermal analysis of a female breast with tumour. J Eng Med 215:25–37

42. Ng EYK, Sudharsan NM (2001) Numerical uncertainty and perfusion induced instability in bioheat equation: its importance in thermographic interpretation. J Med Eng Technol 25:222–229

43. Ng EYK, Sudharsan NM (2004) Computer simulation in conjunction with medical thermography as an adjunct tool for early detection of breast cancer. BMC Cancer 4:17

44. Ng EYK, Fok SC, Peh YC, Ng FC, Sim LSJ (2002) Computerized detection of breast cancer with artificial intelligence and thermograms. J Med Eng Technol 26:152–157

45. Ng EYK, Sudharsan NM (2001) Numerical computation as a tool to aid thermographic interpretation. J Med Eng Technol 25:53–60

46. Nicholson BT, LoRusso AP, Smolkin M, Bovbjerg VE et al (2006) Accuracy of assigned BI-RADS breast density category definitions. Acad Radiol 13:1143–1149

47. Nilsson AL (1987) Blood flow, temperature, and heat loss of skin exposed to local radiative and convective cooling. J Invest Dermatol 88:586–593

48. Osman MM, Afify EM (1984) Thermal modeling of the normal woman's breast. J Biomech Eng 106:123–130

49. Osman MM, Afify EM (1988) Thermal modeling of the malignant woman's breast. J Biomech Eng 110:269–276

50. Pennes HH (1948) Analysis of tissue and arterial blood temperatures in the resting human forearm. J Appl Physiol 85:5–34

51. Saarenmaa I, Salminen T, Geiger U, Heikkinen P et al (2001) The effect of age and density of the breast on the sensitivity of breast cancer diagnostic by mammography and ultasonography. Breast Cancer Res Treat 67:117–123

52. Salim MIM, Supriyanto E, Haueisen J, Ariffin I et al (2013) Measurement of bioelectric and acoustic profile of breast tissue using hybrid magnetoacoustic method for cancer detection. Med Biol Eng Comput 51:459–466

53. Smart CR, Hendrick RE, Rutledge JH, Smith RA (1995) Benefit of mammography screening in women ages 40 to 49 years: current evidence from randomized controlled trials. Cancer 75:1619–1626

54. Sree SV, Ng EYK, Acharya RU, Faust O (2011) Breast imaging: a survey. World J Clin Oncol 2:171–178

55. Sudharsan NM, Ng EYK (2000) Parametric optimization for tumour identification: bioheat equation using ANOVA and the Taguchi method. Proc Inst Mech Eng H 214:505–512

56. Sudharsan N, Ng EYK, Teh SL (1998) Surface temperature distribution of a breast with and without tumour. Comput Methods Biomech Biomed Eng 2:187–199

57. Sudharsan NM, Ng EYK, Teh SL (2007) Surface temperature distribution of a breast with and without tumour. Comput Methods Biomech Biomed Eng 2:187–199

58. Tabar L, Fagerberg G, Chen HH, Duffy SW et al (1995) Efficacy of breast cancer screening by age: new results from the Swedish two-county trial. Cancer 75:2507–2517

59. Umadevi V, Jaipurkar S, Raghavan S (2011) Framework for estimating tumour parameters using thermal imaging. Indian J Med Res 134:725

60. Vreugdenburg TD, Willis CD, Mundy L, Hiller JE (2013) A systematic review of elastography, electrical impedance scanning, and digital infrared thermography for breast cancer screening and diagnosis. Breast Cancer Res Treat 137:665–676

61. Werner J, Buse M (1988) Temperature profiles with respect to inhomogeneity and geometry of the human body. J Appl Physiol 65:1110–1118

62. Zhang S, Gao J (2012) Studying on the thermal conductivity measurement of biological tissues. ECICE 2012, AISC 146:743–749

Asnida A. Wahab received her MEng (EE) degree from the University of Bristol, UK. Currently, she is a Ph.D. candidate and her current research focuses on breast cancer diagnosis advancement using non-invasive thermography technique.

Maheza Irna Mohamad Salim received her Ph.D. in biomedical engineering from University of Technology Malaysia and she is currently holding a senior lecturer post at the same institution. Her research area includes medical imaging and diagnostic, artificial intelligence, and clinical instrumentations.

Mohamad Asmidzam Ahamat obtained his Ph.D. from the University of Bristol, UK. His research includes adsorption heat pumps, heat and mass transfer, thermofluids, and green technology.

Noraida A. Manaf received her Master of Health Science from the National University of Malaysia. She is currently a doctorate candidate, and her research interest is on thermal therapy monitoring using ultrasound technique.

Jasmy Yunus currently holds a position as a Dean of the Faculty of Bioscience and Medical Engineering, UTM. He obtained his Ph.D. in Medical Electronics from the University of Kent in 1992.

Khin Wee Lai obtained his BE and Ph.D. degrees in the field of biomedical engineering. Currently, he is working as a senior lecturer in the Biomedical Engineering Department at University Malaya.